

# 000 001 002 003 004 005 006 007 008 009 010 011 012 013 014 015 016 017 018 019 020 021 022 023 024 025 026 027 028 029 030 031 032 033 034 035 036 037 038 039 040 041 042 043 044 045 046 047 048 049 050 051 052 053 GEOEVOLVE: AUTOMATING GEOSPATIAL MODEL DISCOVERY VIA MULTI-AGENT LARGE LANGUAGE MODELS

Anonymous authors

Paper under double-blind review

## ABSTRACT

Geospatial modeling provides critical solutions for pressing global challenges such as sustainability and climate change. Existing large language model (LLM)-based algorithm discovery frameworks, such as AlphaEvolve, excel at generic code evolution but lack the domain knowledge required for complex geospatial problems. We introduce GeoEvolve, a multi-agent LLM framework that couples evolutionary search with dynamic geospatial domain knowledge. GeoEvolve operates in nested loops: an inner code evolver generates candidate solutions, while an outer agentic controller—supported by Automated Knowledge Construction and Code-to-Formula agents—queries a Dynamic GeoKnowRAG module to inject theoretical priors. This architecture addresses the challenges of spatial heterogeneity and temporal non-stationarity. We evaluate GeoEvolve on three classical tasks: spatial interpolation (Kriging), uncertainty quantification (GeoCP), and spatial regression (GWR). Across 9 datasets, GeoEvolve discovers novel algorithms that incorporate geospatial theory. It achieves significant gains, such as a 29.5% increase in regression  $R^2$  and a 13–21% reduction in interpolation error. Furthermore, extensive ablation studies confirm GeoEvolve’s robustness across diverse foundation models (GPT, Gemini, Qwen) and its spatiotemporal generalizability, validating that domain-guided retrieval is essential for stable evolution. Collectively, these results offer a scalable path toward trustworthy, automated geospatial modeling, opening new avenues for efficient AI-for-Science discovery.

## 1 INTRODUCTION

Beyond building powerful AI models that help us analyze data and understand the world, enabling AI models to evolve on their own and autonomously extract knowledge stands as the next important and promising frontier. It usually involves a prolonged procedure of asking a research question, gathering relevant information, analyzing it to identify patterns or insights, and communicating the results as new knowledge. The rise of the large language models (LLMs), such as GPT-4 (Achiam et al., 2023) and Gemini (Comanici et al., 2025), presents the possibility of accelerating and automating this knowledge discovery procedure. The confidence in this direction is supported by the breakthroughs in LLMs, such as retrieval augmented generation (RAG) that enhances the output of LLMs (Lewis et al., 2020; Jiang et al., 2023) and agents that execute complex tasks autonomously (Li et al., 2023; Qian et al., 2024). In fact, the integration of LLMs into this procedure has already boosted the performance of a range of discovery-oriented tasks, such as drug repurposing (Huang et al., 2024), hypothesis generation (Kumbhar et al., 2025; Xiong et al., 2024), chip design (Ho & Ren, 2024), urban planning (Zhou et al., 2024). Recently, Google introduced AlphaEvolve, which has demonstrated remarkable capabilities in automating algorithm discovery across diverse domains, such as tackling complex mathematical optimization problems. Building on this foundation, OpenEvolve has been developed as an open-source implementation of Google DeepMind’s AlphaEvolve, providing the research community with accessible tools for further exploration and application.

Despite these advances, the domain of geospatial modeling remains relatively underexplored in the context of LLM-driven knowledge discovery. Geospatial problems are inherently complicated,

054 characterized by spatial autocorrelation (Miller, 2004), spatial heterogeneity (Cheng et al., 2024),  
 055 scale effect (Chen et al., 2019), and diverse modalities (e.g., maps, remote sensing imagery, spatial  
 056 network, and textual description) (Mai et al., 2023), etc. Moreover, addressing geospatial problems  
 057 also demands synthesizing knowledge across different disciplines, from environmental science to  
 058 urban studies, making it difficult for single-agent systems to provide comprehensive solutions.

059 In this paper, we introduce GeoEvolve, an advanced agent combining the evolutionary process with  
 060 LLM-based code generation and geospatial knowledge-informed RAG (GeoKnowRAG) to automatically  
 061 investigate optimal geospatial modeling. GeoEvolve operates in two complementary loops.  
 062 As is shown in Figure 1, the inner loop runs OpenEvolve (Sharma, 2025) for a limited number of  
 063 evolutionary steps, generating candidates of discovery. The outer loop is governed by an agentic  
 064 controller, which evaluates the best solutions, retains global elites to prevent performance degra-  
 065 dation, and invokes the GeoKnowRAG module. This module will query a structured geospatial  
 066 knowledge database, thus producing refined, domain-informed prompts that guide the next round  
 067 evolution. We show that GeoEvolve can obviously improve the geospatial modeling.

068 In summary, the contributions of our work are as follows:  
 069

- 070 **Knowledge-guided evolution.** We integrate evolutionary search with domain knowledge  
 071 by coupling GeoEvolve’s evolutionary code generation (via OpenEvolve) with retrieval-  
 072 augmented geospatial knowledge. This grounds discovery in established geospatial theo-  
 073 ries and classical methods rather than random mutations, steering evolution toward theo-  
 074 retically meaningful and practically effective directions.
- 075 **Automated, scalable pipeline.** We develop an automated and scalable geospatial modeling  
 076 pipeline that can continuously evolve, adapt, and refine geospatial algorithms, providing a  
 077 robust methodology for diverse geospatial tasks.
- 078 **State-of-the-art performance and efficiency.** We demonstrate state-of-the-art perfor-  
 079 mance on two spatial modeling cases—spatial interpolation and spatial uncertainty quan-  
 080 tification—supported by an ablation study verifying the role of domain knowledge.

## 082 2 RELATED WORK

084 **LLM-driven Algorithm Discovery** Driven by LLMs, many studies aim to accelerate the dis-  
 085 covery of algorithms with better performance, simpler implementation, and higher computational  
 086 efficiency. A common approach is evolutionary search, which explores the algorithmic space via  
 087 mutations and recombinations guided by performance metrics (Surina et al., 2025), enabling break-  
 088 throughs across diverse applications (Lu et al., 2024; Ma et al., 2024; Veličković et al., 2024; Mor-  
 089 ris et al., 2024). Among the most influential methods is FunSearch—searching in the function  
 090 space—which fosters creative algorithmic solutions while guarding against confabulations (Romera-  
 091 Paredes et al., 2024), but is limited to evolving a single function rather than an entire codebase.  
 092 AlphaEvolve, a substantially enhanced successor, leverages LLMs to solve complex problems at  
 093 scale (Novikov et al., 2025). Yet addressing specialized challenges, particularly in geospatial do-  
 094 mains, requires domain-specific knowledge, multi-step reasoning, and iterative refinement guided  
 095 by evaluation feedback (Chen et al., 2024).

096 **Retrieval-augmented generation RAG for scientific discovery.** RAG has emerged as a standard  
 097 strategy to ground LLM outputs in external knowledge, improving factual accuracy and controllabil-  
 098 ity (Lewis et al., 2020; Gao et al., 2023). Recent advances such as RAG-Fusion (Rackauckas, 2024)  
 099 and reciprocal rank fusion (RRF) (Cormack et al., 2009) demonstrate that expanding and fusing mul-  
 100 tiple reformulated queries can substantially enhance retrieval coverage and downstream reasoning  
 101 quality. Moreover, RAG has recently been applied in the geospatial domain to support knowledge  
 102 discovery and contribute to downstream tasks such as spatial reasoning (Yu et al., 2025). However,  
 103 to the best of our knowledge, no prior work has leveraged RAG to extract geospatial knowledge  
 104 specifically for geospatial model construction, leaving an important gap for integrating structured  
 105 geographic knowledge into model design.

106 **LLM-based Autonomous Agents** Recent advances in LLM-based autonomous agents have sub-  
 107 stantially expanded their capacity for solving complex tasks through multi-agent collaboration and

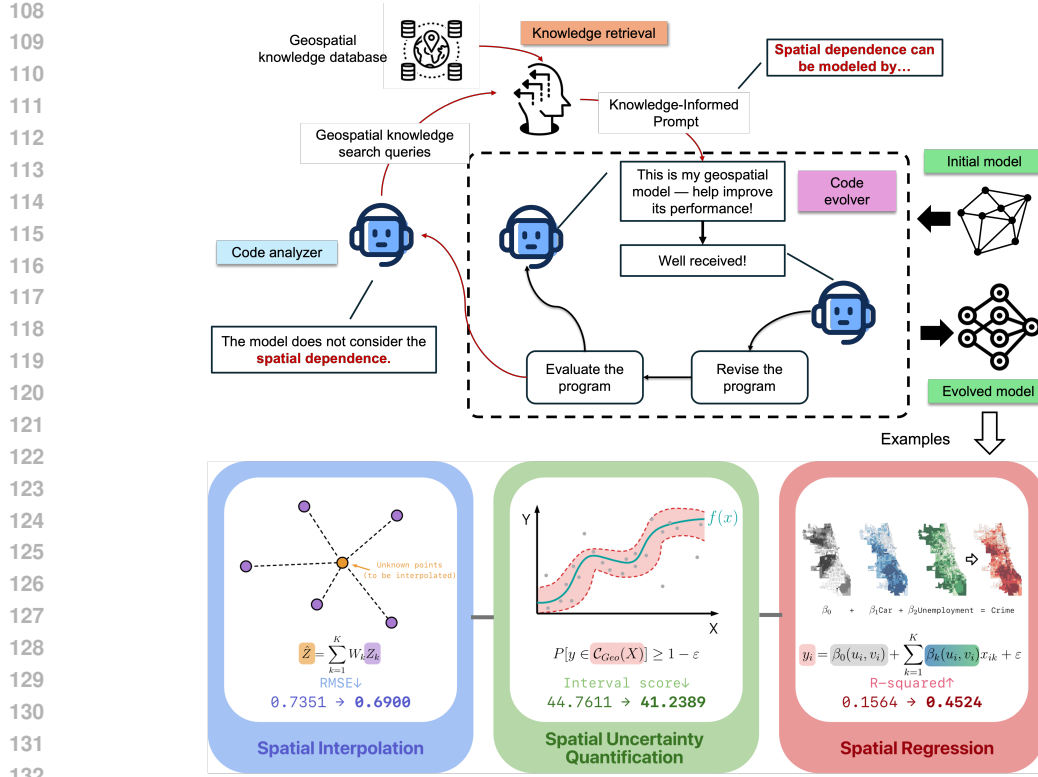


Figure 1: An illustration of the code-evolution trajectory of a geospatial model integrating domain knowledge. The dashed inner box represents the code evolver, a general algorithmic code-generation engine. The surrounding workflow depicts the knowledge-guided code generation proposed in this paper, specifically tailored for geospatial modeling.

structured role-playing (Wang et al., 2024). Frameworks such as MetaGPT (Hong et al., 2023) and ChatDev (Qian et al., 2024) emulate the Standard Operating Procedures of software companies, assigning roles such as product managers and engineers to automate large portions of the software development lifecycle. In the geography domain, LLM-based agents have also been introduced to automate geospatial modeling workflows—including data ingestion, processing, analysis, and visualization—greatly lowering the technical barrier for using domain-specific tools (Li & Ning, 2023). However, while these systems are highly effective at executing linear engineering workflows with well-defined requirements, they are generally not designed for scientific discovery, which requires open-ended objectives, evolving hypotheses, and exploration within large and uncertain search spaces.

### 3 GEOEVOLVE

GeoEvolve is designed to automate geospatial model discovery by integrating evolutionary code generation with structured geospatial knowledge. Unlike general-purpose code agents, GeoEvolve incorporates domain-specific knowledge from spatial modeling literature and classical algorithms, enabling the discovery of geospatial algorithms. Figure 2 illustrates the overall framework of GeoEvolve. It consists of four main components: (1) a code evolver, (2) an evolved code analyzer, (3) a geospatial knowledge retriever, and (4) a geo-informed prompt generator. Together, these components orchestrate a closed-loop process of code generation, evaluation, and refinement, leading to the emergence of geospatial model discovery.

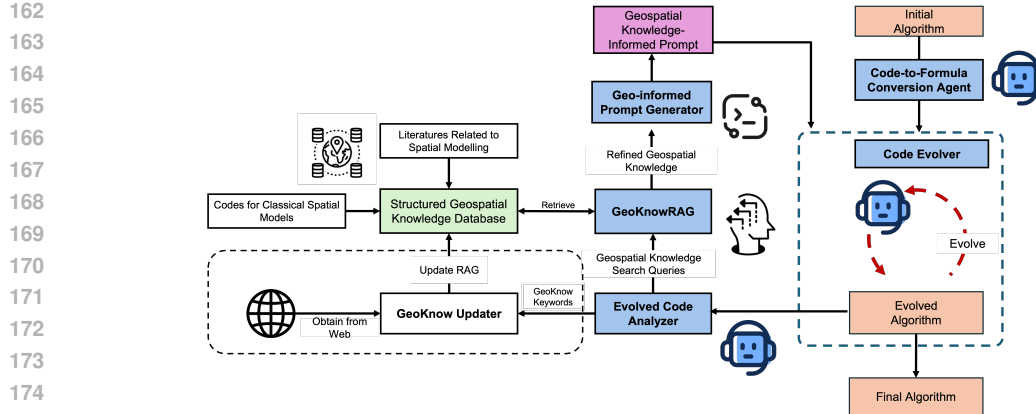


Figure 2: The workflow of GeoEvolve

### 3.1 CODE-TO-FORMULA AGENT

To streamline the transition from user-defined geospatial models to evolutionary search spaces, GeoEvolve incorporates an Code-to-Formula agent. Instead of requiring users to manually configure the complex input specifications—comprising the initial program, evaluator logic, and instructional prompts—this agent employs an LLM-based semantic parser to automate the initialization process.

Guided by a set of pre-defined heuristic templates and few-shot exemplars derived from classical geospatial algorithms (e.g., Kriging, GeoCP), the agent analyzes the user’s raw code to extract core algorithmic logic. It then encapsulates this logic into a standardized triplet format required by the evolutionary engine. This design effectively decouples the user’s domain implementation from the framework’s internal search protocols, allowing researchers to focus on model logic rather than configuration details. These standardized templates and illustrative exemplars are encapsulated as built-in assets within the GeoEvolve codebase, enabling an out-of-the-box experience for users.

### 3.2 CODE EVOLVER

The central engine of GeoEvolve is the code evolver, an evolutionary coding agent that generates and iteratively refines candidate algorithms. Beginning with an initial algorithm, the evolver performs a fully autonomous pipeline of mutation, evaluation, and selection relying on the power of LLMs. Candidate algorithms are represented as a group of executable code fragments. Mutations can be parameter changes, operator substitutions, or structure modifications to the algorithm. Abstractly, given a task-specific objective function  $\mathcal{L}$ , the evolver seeks to optimize an algorithm  $A$  such that

$$A^* = \arg \min_{A \in \mathcal{A}} \mathcal{L}(A; \mathcal{D}), \quad (1)$$

where  $\mathcal{A}$  is the search space and  $\mathcal{D}$  is the dataset. Here, we use OpenEvolve as the code evolver, which is the open-source equivalent of AlphaEvolve.

### 3.3 EVOLVED CODE ANALYZER

The evolved code analyzer is an LLM-powered diagnostic agent that interprets both the evolved code and associated metrics (e.g., RMSE for regression tasks). Its role is not limited to evaluating task outcomes, but also to providing semantic analysis of the code, thus identifying potential weaknesses or missing knowledge. To be specific, the LLM is required to achieve two tasks. First, it identifies missing or problematic knowledge from the evolved code. Second, it suggests search queries for retrieving useful geospatial knowledge from GeoKnowRAG. The diagnostic feedback given by this agent will be passed to the geospatial knowledge retriever to obtain related knowledge. This design allows GeoEvolve to reason about why the evolved algorithm fails and what kind of domain knowledge is needed to improve it. The template and an example of the code analyzer can be found at Figure 6.

216 3.4 GEOSPATIAL KNOWLEDGE RETRIEVER  
217

218 To prevent the evolutionary search from drifting into non-meaningful algorithmic space, GeoEvolve  
219 incorporates domain-specific geospatial knowledge through a dedicated Geospatial Knowledge Re-  
220 trieval module (GeoKnowRAG). We construct a structured knowledge base by collecting literature  
221 on core geospatial modeling concepts (e.g., spatial autocorrelation) and classical algorithms (e.g.,  
222 geographically weighted regression) from Wikipedia, arXiv, and GitHub, using curated keywords  
223 (Figure 7, Appendix A.3.1). To ensure high-quality and comprehensive knowledge coverage, RAG-  
224 Fusion (Rackauckas, 2024) is applied to merge results from multiple reformulated queries, enabling  
225 the system to capture both precise theoretical matches and semantically related concepts. Geo-  
226 KnowRAG transforms these diverse resources into a structured RAG system that delivers domain-  
227 aware prompts directly to the code evolver, providing the theoretical grounding and classical geospatial  
228 methods required for effective algorithmic refinement. As shown in Figure 3, GeoKnowRAG  
229 comprises four steps:

230 **Source Identification and Acquisition** Unlike previous approaches that rely on manually curated  
231 static topic lists, GeoEvolve employs a fully automated, agent-driven pipeline to construct and con-  
232 tinuously evolve its knowledge base. This process operates in two phases: automated initialization  
233 and dynamic expansion.

234 First, to establish the foundational knowledge base, we introduce an Automated Knowledge Base  
235 Construction Agent. Upon receiving the user’s baseline geospatial code, this agent performs seman-  
236 tic analysis to extract core algorithmic concepts and automatically identifies an initial set of search  
237 keywords (defaulting to 5 key terms). These keywords drive the initial retrieval from three comple-  
238 mentary corpora—peer-reviewed papers (arXiv), encyclopedic entries (Wikipedia), and open-source  
239 repositories (GitHub)—downloading up to 150 documents to form a task-specific, normalized UTF-  
240 8 knowledge repository.

241 Second, to address theoretical gaps that emerge during evolution, we implement a Dynamic Knowl-  
242 edge Update loop. In each outer iteration, the Evolved Code Analyzer scrutinizes the evolved code  
243 and performance metrics. Acting as a diagnostic gatekeeper, it determines whether the current al-  
244 gorithmic bottleneck stems from a lack of domain knowledge. If a deficit is identified, the agent  
245 generates precise search queries and triggers the GeoKnow Updater, which fetches high-relevance  
246 literature from the web (capped at 5 new documents per cycle) to augment the database in real-time.  
247 Conversely, if the knowledge base is deemed sufficient, the system adaptively reverts to static re-  
248 trieval to conserve resources. Finally, the Geo-informed Prompt Generator synthesizes the updated  
249 knowledge with the current code to steer the next evolutionary step.

250 **Text Chunking and Pre-processing** First, each document is semantically segmented into 300-  
251 word chunks with a 50-word overlap to preserve contextual continuity across chunk boundaries  
252 and improve downstream retrieval accuracy. Second, all PDF, Markdown, and HTML sources are  
253 stripped of formatting, de-duplicated, and tokenized into a clean corpus ready for embedding.

254 **Vectorization and Knowledge Indexing** First, every chunk is encoded using the  
255 text-embedding-3-small model from OpenAI to obtain high-dimensional semantic  
256 vectors. Second, these embeddings are stored in a **Chroma** vector database, which supports  
257 approximate nearest-neighbor search and metadata filtering by topic or source type. Third, this  
258 indexed database forms the persistent memory of GeoKnowRAG and enables millisecond-scale  
259 retrieval across the geospatial knowledge space.

260 **RAG-Fusion Query and Prompt Generation** First, GeoKnowRAG employs multi-angle ques-  
261 tion expansion, where each input query from the GeoEvolve controller is reformulated into several  
262 sub-questions emphasizing different semantic aspects such as theory, implementation, and evalua-  
263 tion. Second, each sub-question is independently embedded and used for vector search to retrieve  
264 top- $k$  relevant chunks from the Chroma index. Third, the retrieved results are re-ranked using RRF,  
265 which scores passages based on the reciprocal of their ranks across sub-queries so that consistently  
266 high-scoring chunks surface to the top. Fourth, the highest-ranked passages are aggregated and  
267 summarized into a geo-informed prompt encoding key formulas, algorithmic structures, and empir-

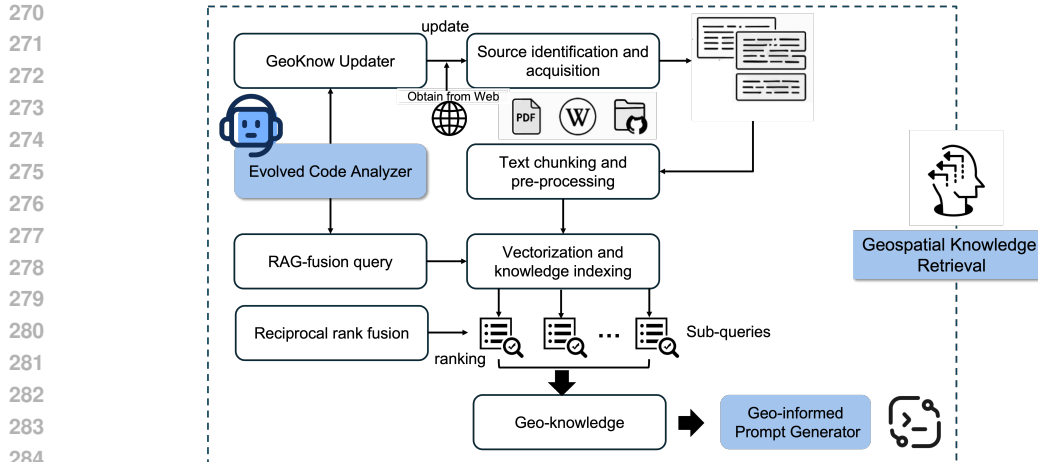


Figure 3: The workflow of GeoKnowRAG

ical heuristics, which is then supplied to the GeoEvolve code evolver to guide the next round of algorithmic mutation and evaluation.

### 3.5 GEO-INFORMED PROMPT GENERATOR

The information, from retrieved geospatial knowledge to evolved code, and associated metrics, is then processed together by the geo-informed prompt generator, which will translate it into a structured prompt for the code evolver. This prompt refines the search by introducing domain constraints, suggesting algorithmic structures, or incorporating empirical heuristics. The generator leverages LLMs as reasoning and translation engines, transforming abstract geospatial knowledge into actionable modifications of candidate code.

The LLMs are required to generate a prompt that includes four key elements. First, algorithmic fixes or improvements suggesting how the current algorithm could be revised. Second, new operators or parameters that may improve performance in subsequent evolutionary iterations. Third, geospatial knowledge, including the direction of exploration, theoretical or empirical conditions, and expected outputs. Fourth, maximum tokens control, which helps maintain efficiency and reduce hallucination.

## 4 EXPERIMENTS

To evaluate GeoEvolve’s capability for improving and discovering geospatial models, we focus on three fundamental topics: spatial interpolation, uncertainty quantification, and spatial regression. We detail the first two in the main text and present the spatial regression results in Appendix. For each topic, we select the most representative and classical baseline model, and employ a GPT-4-based evolutionary engine as the core evolve agent to autonomously search, mutate, and refine candidate algorithms.

We use OpenEvolve as the primary baseline. In addition, we conduct an ablation study with two variants. First, OpenEvolve with GeoKnowledge Prompt, where domain knowledge is incorporated as additional prompts. The prompt template is: “*You are allowed to refer to advanced methods in the field of spatial interpolation and consider some important settings of spatial models, such as localized variogram, automatic variogram parameter selection, or stratified strategy, etc.*” Second, GeoEvolve without GeoKnowledge, where the GeoKnowRAG module is removed. For every algorithm, after each evolutionary step the generated code is first analyzed by the code analyzer and then directly passed to the knowledge-prompt generator to create new prompts.

For the OpenEvolve-based algorithms, we perform ten iterations of evolutionary search. For the GeoEvolve algorithms, we run ten outer-loop cycles—each consisting of the code analyzer, GeoKnowRAG, and geo-informed prompt generator—and within every outer cycle we conduct ten

324 inner-loop evolutions. This results in a total of one hundred evolutionary iterations. For every  
 325 experiment, the dataset is split into training, validation, and test sets in an 8:1:1 ratio.  
 326

327 **Crucially, we extend our evaluation to the unique challenge of geospatial generalizability, testing**  
 328 **the framework across 9 datasets. Geospatial modeling demands robustness across three dimensions:**  
 329 **Domain Generalizability (transferring logic between disparate fields, e.g., socioeconomic vs. en-**  
 330 **vironmental data), Spatial Generalizability (adapting to spatial heterogeneity across regions), and**  
 331 **Temporal Generalizability (mitigating non-stationarity over time).**

#### 332 4.1 SPATIAL INTERPOLATION MODEL

333 **Task- Spatial interpolation** Spatial interpolation is one of the most important applications in  
 334 geospatial analysis and a key approach for humans to observe the Earth’s surface environment and  
 335 understand the planet (Lam, 1983). Its task is to model discrete sample points collected across  
 336 geographic space—such as climate observation stations, biodiversity observation points, or mineral  
 337 sampling sites—and to predict the continuous spatial surface of the geographic variables of interest  
 338 based on these observations.  
 339

340 **Model- Ordinary Kriging** We selected ordinary kriging, the most classical geostatistical spatial  
 341 interpolation model, as the first case study for GeoEvolve to automatically improve and evaluate.  
 342 Since its invention, many studies have attempted to extend kriging, for example by integrating re-  
 343 gression models in regression kriging (Hengl et al., 2007) or by accounting for spatially stratified  
 344 heterogeneity in stratified kriging (Luo et al., 2023). However, ordinary kriging remains the funda-  
 345 mental core of the entire kriging family and of geostatistics itself. Because it was developed long  
 346 ago and has a relatively simple structure, direct algorithmic innovations to ordinary kriging have  
 347 become increasingly rare. More details about ordinary kriging can be found at Appendix A.3.1.  
 348

349 If GeoEvolve can demonstrably enhance ordinary kriging, it would greatly revitalize geostatistical  
 350 methods and provide fundamental improvements that can propagate to all kriging-based models and  
 351 applications. This rationale underpins our choice of ordinary kriging as the first benchmark algorithm  
 352 in this study.

353 **Evaluator** For the kriging interpolation task, we use the root mean squared error (RMSE) as the  
 354 evaluation metric. Our objective is to obtain a kriging model that achieves a lower RMSE, indicating  
 355 higher predictive accuracy.  
 356

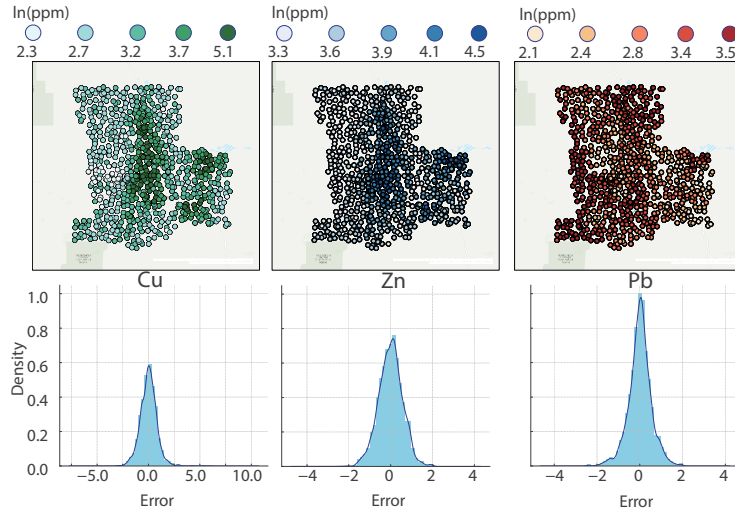
357 **Datasets** In this study, we use trace-element observations of copper (Cu), lead (Pb), and zinc  
 358 (Zn) collected from a representative region of Australia (with concentrations expressed in parts per  
 359 million, ppm) to conduct spatial interpolation and geostatistical modeling experiments. These three  
 360 heavy metals have important indicative significance in environmental geochemistry: on the one  
 361 hand, they serve as key factors for assessing regional environmental pollution levels and soil heavy-  
 362 metal accumulation. Details of the data acquisition and processing procedures can be found in (Luo  
 363 et al., 2025).  
 364

##### 365 4.1.1 EVOLVED ALGORITHM OF ORDINARY KRIGING.

366 GeoEvolve preserves the ordinary-kriging core but augments it with (i) an expanded variogram  
 367 family (Exponential, Gaussian, Linear, and Matérn) with automatic model selection via AIC/BIC,  
 368 capturing a wider range of spatial smoothness; (ii) an adaptive empirical variogram using quan-  
 369 tile/Silverman binning, trimmed means, and an automatic  $n_{\text{lags}} \in [8, 20] \propto \sqrt{n}$  to stabilize  
 370 nugget/sill/range estimation; (iii) robust multi-start fitting with L1 or weighted least squares and  
 371 bin-based weights to avoid local minima and keep parameters physically meaningful; (iv) localized  
 372 kriging that solves a  $K$ -NN system with condition-number-aware diagonal adjustment, reducing  
 373 complexity from  $O(n^3)$  to  $O(K^3)$  and improving numerical stability; and (v) an adaptive log trans-  
 374 form with a data-driven offset to reduce skew and ensure valid back-transformation. Together, these  
 375 changes retain unbiasedness and best-linear prediction while delivering lower RMSE/MAE, tighter  
 376 residuals, and greater computational robustness across heterogeneous spatial settings. The detailed  
 377 development of GeoEvolve–Kriging can be found at Appendix A.4.1.

378 Table 1: Performance comparison across different methods. For each metal, lower is better for  
 379 RMSE/MAE, and higher is better for  $R^2$ .  
 380

381 Method	382 Cu			383 Pb			384 Zn		
	385 RMSE ↓	386 MAE ↓	387 $R^2 \uparrow$	388 RMSE ↓	389 MAE ↓	390 $R^2 \uparrow$	391 RMSE ↓	392 MAE ↓	393 $R^2 \uparrow$
Original	0.9139	0.6752	0.3751	0.6619	0.4580	0.3563	0.6294	0.4689	0.4304
OpenEvolve (No GeoKnowledge)	0.8727	0.6557	<b>0.4302</b>	0.6413	0.4441	<b>0.3957</b>	0.6245	0.4712	0.4395
OpenEvolve (General GeoKnowledge)	0.9264	0.6519	0.3755	0.6519	0.4598	0.3755	0.6332	0.4725	0.4235
OpenEvolve (Specific GeoKnowledge)	0.9139	0.6761	0.3752	0.6632	0.4579	0.3537	0.6337	0.4716	0.4227
GeoEvolve (No RAG))	0.9139	0.7321	0.2889	0.6619	0.5871	0.0298	0.6294	0.5905	0.1723
GeoEvolve (Static RAG))	0.8602	0.6423	0.3596	0.5927	0.4390	0.3025	0.5941	0.4475	<b>0.4433</b>
GeoEvolve (Dynamic RAG)	<b>0.8718</b>	<b>0.6418</b>	0.3721	<b>0.6131</b>	<b>0.4299</b>	0.3492	<b>0.5852</b>	<b>0.4388</b>	0.4363



410 Figure 4: The spatial distribution of predicted concentrations and the error distribution of three  
 411 elements, Cu, Zn, and Pb obtained from Evolved Kriging

#### 412 4.1.2 MODEL EVALUATION

413  
 414  
 415 Table 1 reports the kriging accuracy obtained by different methods. GeoEvolve-kriging consistently  
 416 achieves the lowest RMSE and MAE across the prediction of Cu, Pb, and Zn, while the original kriging  
 417 baseline performs worst. Applying OpenEvolve to kriging improves the prediction of Cu and Pb  
 418 but slightly degrades the performance on Zn. Introducing GeoKnowledge prompts into OpenEvolve  
 419 does not lead to further gains, possibly because the injected knowledge lacks direct relevance to  
 420 variogram estimation or spatial covariance structures that govern kriging performance. GeoEvolve  
 421 without GeoKnowRAG already outperforms OpenEvolve, yet still falls short of the full GeoEvolve  
 422 model, underscoring the critical role of structured geospatial domain knowledge in guiding algo-  
 423 rithm evolution.

424  
 425 Compared with OpenEvolve-kriging, GeoEvolve-kriging reduces RMSE by 11.3%, 20.9%, and  
 426 13.5% on Cu, Pb, and Zn predictions, respectively. Relative to the original kriging, the reductions  
 427 are 15.4%, 21.2%, and 13.0%, further highlighting GeoEvolve’s ability to automatically discover  
 428 and refine spatial interpolation algorithms with substantially improved predictive accuracy.

429  
 430 Figure 4 illustrates the spatial distributions of the predicted concentrations and the associated error  
 431 maps for Cu, Pb, and Zn obtained by GeoEvolve-kriging, clearly demonstrating its capability to  
 432 capture fine-scale spatial variability while maintaining low residual errors.

432 4.2 SPATIAL UNCERTAINTY QUANTIFICATION MODEL  
433

434 **Task- Spatial UQ** In spatial predictive modeling, it is not sufficient merely to develop more accurate models for point predictions; an equally critical task is to quantify and communicate the uncertainty of predictions, as this directly shapes the reliability and legitimacy of geography-based decisions such as flood evacuation planning and public facility site selection. Therefore, incorporating rigorous uncertainty quantification into spatial prediction is essential not only for improving scientific credibility, but also for supporting transparent, fair, and ethically sound spatial planning and policy making.

441 **Model- GeoCP** In geography, the task of assessing the reliability of spatial prediction results is commonly addressed through uncertainty quantification (UQ). In this study, we adopt geospatial conformal prediction (GeoCP)—a model-agnostic algorithm for estimating the uncertainty of spatial prediction models—as the target method for enhancement using GeoEvolve (Lou et al., 2025b). More details about GeoCP can be found at Appendix A.3.2.

447 **Evaluator** For GeoCP uncertainty estimation, we use the *interval score*

$$449 \quad IS_i = \max(U_i - L_i, \epsilon) + \frac{2}{\alpha} [(L_i - y_i)\mathbb{I}(y_i < L_i) + (y_i - U_i)\mathbb{I}(y_i > U_i)], \quad (2)$$

451 where  $L_i, U_i$  are prediction bounds,  $y_i$  the observation, and  $\alpha$  the significance level (e.g., 0.1 for 452 90% intervals). The first term measures interval width (with  $\epsilon \approx 10^{-6}$  to avoid zero width), and 453 the second penalizes coverage violations, scaled by  $1/\alpha$ . Smaller IS indicates tighter and better- 454 calibrated intervals.

456 **Datasets** The housing price dataset used in this study originates from the GeoDa Lab repository<sup>1</sup>. 457 The original data include 21,613 residential transactions and 21 attributes from Seattle and King 458 County, Washington (May 2014–May 2015). For our analysis, we focus on the Greater Seattle urban 459 core and retain 11 key variables, with housing sale price (in \$10,000s) as the dependent variable. 460 Eight non-spatial predictors capture structural and quality characteristics—bathrooms, living-space 461 and lot size, grade, condition, waterfront proximity, view quality, and property age—while two 462 spatial predictors are geographic coordinates expressed in UTM (universal transverse mercator). 463 Further details of the dataset are documented in (Lou et al., 2025b;a).

464 4.2.1 EVOLVED ALGORITHM OF GEOCP  
465

466 GeoEvolve–GeoCP preserves the fundamental conformal prediction framework of GeoCP while 467 introducing two major methodological advances. First, it refines the geographic weighting scheme: 468 still employing a Gaussian kernel, but re-optimizing the bandwidth parameter through multi-start 469 global search with adaptive clipping to ensure numerical stability and faithfully capture local spatial 470 heterogeneity. Second, it enhances the weighted quantile computation by unifying earlier adaptive 471 strategies into a simplified yet robust stepwise estimator with improved vectorization and conditioning 472 checks, thereby delivering higher accuracy and better scalability on large test sets. The detailed 473 analysis of GeoEvolve–GeoCP can be found at Appendix A.4.2.

474 4.2.2 MODEL EVALUATION  
475

476 To perform GeoCP, we first build a house-price prediction model using a base predictor with eight 477 explanatory variables and two spatial variables as inputs. The trained model is then assessed with 478 GeoCP to quantify predictive uncertainty, and the final output is the uncertainty of house-price 479 predictions on the test set. In this study, we choose XGBoost as the base predictor, which achieves 480 an  $R^2$  of 0.871 and an RMSE of 7.362 (10,000 USD). The results are presented in Figure 5. The 481 predicted uncertainty exhibits a clear spatial pattern: it is highest around Lake Washington in 482 downtown Seattle, slightly lower in suburban areas, and lowest in the rural southern region. A scatter plot 483 of predicted uncertainty versus predicted price further reveals that uncertainty increases with house 484 price, peaking at approximately 125 (10,000 USD) and then leveling off with a slight decline.

485 <sup>1</sup><https://geodacenter.github.io/data-and-lab/KingCounty-HouseSales2015/>

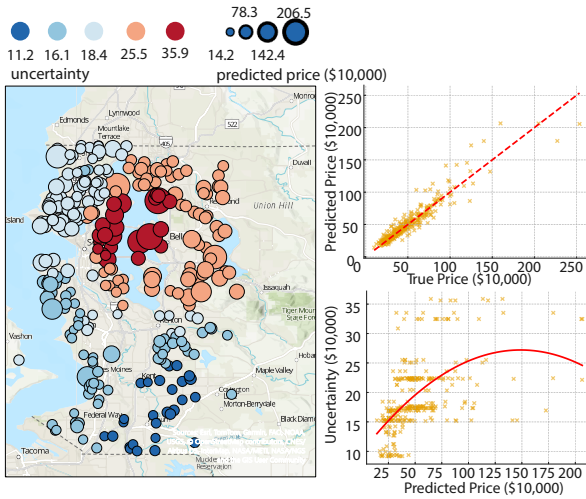


Figure 5: The spatial distribution of estimated uncertainty for the housing price prediction task in Seattle using the evolved GeoCP.

Table 2: Comparison of conformal prediction metrics. Smaller Average Interval Size and Interval Score indicate sharper and more efficient intervals.

Method	Average Interval Size ↓	Interval Score ↓
Original	18.3254	44.7611
OpenEvolve (No GeoKnowledge)	16.9139	43.1823
OpenEvolve (General GeoKnowledge)	17.1508	42.8343
OpenEvolve (Specific GeoKnowledge)	13.9557	41.4267
GeoEvolve (No RAG)	17.5586	44.2545
GeoEvolve (Static RAG)	18.5818	45.2738
GeoEvolve (Dynamic RAG)	<b>13.7750</b>	<b>41.2389</b>

We apply GeoCP in seven configurations, original, OpenEvolve without GeoKnowledge Prompt, OpenEvolve with General GeoKnowledge Prompt, OpenEvolve with Specific GeoKnowledge Prompt, GeoEvolve without GeoKnowRAG, GeoEvolve with Static GeoKnowRAG, and GeoEvolve with Dynamic GeoKnowRAG—to quantify uncertainty on the same test set. Table 2 reports the GeoCP performance obtained by different methods. As shown, different variants of OpenEvolve reduces the interval score to 43.1823, 42.8343, and 41.4267, respectively. In comparison with OpenEvolve, the three variants of GeoEvolve achieves an interval score of 44.2545, 45.2738, 41.2389, respectively. The performance of GeoEvolve with static GeoKnowRAG even degrades, this may suggest that GeoKnowRAG fails to provide useful geographical knowledge for evolution. However, when dynamically updating new geographical knowledge, GeoEvolve shows unprecedented performance.

## 5 CONCLUSION

We presented GeoEvolve, a multi-agent LLM framework that couples evolutionary code search with geospatial domain knowledge via GeoKnowRAG to automate geospatial model discovery. Across three fundamental tasks, GeoEvolve consistently improved upon classical baselines and strong OpenEvolve variants. Ablations confirm that structured, domain-guided retrieval is pivotal: removing GeoKnowRAG degrades performance despite identical evolutionary budgets, underscoring the value of grounding algorithm evolution in geospatial theory.

540 REFERENCES  
541

542 Josh Achiam, Steven Adler, Sandhini Agarwal, Lama Ahmad, Ilge Akkaya, Florencia Leoni Ale-  
543 man, Diogo Almeida, Janko Altenschmidt, Sam Altman, Shyamal Anadkat, et al. Gpt-4 technical  
544 report. *arXiv preprint arXiv:2303.08774*, 2023.

545 Lei Chen, Yong Gao, Di Zhu, Yihong Yuan, and Yu Liu. Quantifying the scale effect in geospatial  
546 big data using semi-variograms. *PloS one*, 14(11):e0225139, 2019.

547 Yuxing Chen, Weijie Wang, Sylvain Lobry, and Camille Kurtz. An llm agent for automatic geospatial  
548 data analysis. *arXiv preprint arXiv:2410.18792*, 2024.

549 Shifen Cheng, Lizeng Wang, Peixiao Wang, and Feng Lu. An ensemble spatial prediction method  
550 considering geospatial heterogeneity. *International Journal of Geographical Information Science*,  
551 38(9):1856–1880, 2024.

552 Gheorghe Comanici, Eric Bieber, Mike Schaeckermann, Ice Pasupat, Noveen Sachdeva, Inderjit  
553 Dhillon, Marcel Blstein, Ori Ram, Dan Zhang, Evan Rosen, et al. Gemini 2.5: Pushing the  
554 frontier with advanced reasoning, multimodality, long context, and next generation agentic capa-  
555 bilities. *arXiv preprint arXiv:2507.06261*, 2025.

556 Gordon V Cormack, Charles LA Clarke, and Stefan Buettcher. Reciprocal rank fusion outperforms  
557 condorcet and individual rank learning methods. In *Proceedings of the 32nd international ACM  
558 SIGIR conference on Research and development in information retrieval*, pp. 758–759, 2009.

559 A Stewart Fotheringham, Chris Brunsdon, and Martin Charlton. Geographically weighted regres-  
560 sion. *The Sage handbook of spatial analysis*, 1:243–254, 2009.

561 Yunfan Gao, Yun Xiong, Xinyu Gao, Kangxiang Jia, Jinliu Pan, Yuxi Bi, Yixin Dai, Jiawei Sun,  
562 Haofen Wang, and Haofen Wang. Retrieval-augmented generation for large language models: A  
563 survey. *arXiv preprint arXiv:2312.10997*, 2(1), 2023.

564 Tomislav Hengl, Gerard BM Heuvelink, and David G Rossiter. About regression-kriging: From  
565 equations to case studies. *Computers & geosciences*, 33(10):1301–1315, 2007.

566 Chia-Tung Ho and Haoxing Ren. Large language model (llm) for standard cell layout design opti-  
567 mization. In *2024 IEEE LLM Aided Design Workshop (LAD)*, pp. 1–6. IEEE, 2024.

568 Sirui Hong, Mingchen Zhuge, Jonathan Chen, Xiawu Zheng, Yuheng Cheng, Jinlin Wang, Ceyao  
569 Zhang, Zili Wang, Steven Ka Shing Yau, Zijuan Lin, et al. Metagpt: Meta programming for  
570 a multi-agent collaborative framework. In *The Twelfth International Conference on Learning  
571 Representations*, 2023.

572 Kexin Huang, Payal Chandak, Qianwen Wang, Shreyas Havaldar, Akhil Vaid, Jure Leskovec,  
573 Girish N Nadkarni, Benjamin S Glicksberg, Nils Gehlenborg, and Marinka Zitnik. A founda-  
574 tion model for clinician-centered drug repurposing. *Nature Medicine*, 30(12):3601–3613, 2024.

575 Zhengbao Jiang, Frank F Xu, Luyu Gao, Zhiqing Sun, Qian Liu, Jane Dwivedi-Yu, Yiming Yang,  
576 Jamie Callan, and Graham Neubig. Active retrieval augmented generation. In *Proceedings of the  
577 2023 Conference on Empirical Methods in Natural Language Processing*, pp. 7969–7992, 2023.

578 Shrinidhi Kumbhar, Venkatesh Mishra, Kevin Coutinho, Divij Handa, Ashif Iquebal, and Chitta  
579 Baral. Hypothesis generation for materials discovery and design using goal-driven and constraint-  
580 guided llm agents. *arXiv preprint arXiv:2501.13299*, 2025.

581 Nina Siu-Ngan Lam. Spatial interpolation methods: a review. *The American Cartographer*, 10(2):  
582 129–150, 1983.

583 Patrick Lewis, Ethan Perez, Aleksandra Piktus, Fabio Petroni, Vladimir Karpukhin, Naman Goyal,  
584 Heinrich Küttler, Mike Lewis, Wen-tau Yih, Tim Rocktäschel, et al. Retrieval-augmented gener-  
585 ation for knowledge-intensive nlp tasks. *Advances in neural information processing systems*, 33:  
586 9459–9474, 2020.

594 Guohao Li, Hasan Hammoud, Hani Itani, Dmitrii Khizbulin, and Bernard Ghanem. Camel: Com-  
 595 municative agents for “mind” exploration of large language model society. *Advances in Neural*  
 596 *Information Processing Systems*, 36:51991–52008, 2023.

597

598 Zhenlong Li and Huan Ning. Autonomous gis: the next-generation ai-powered gis. *International*  
 599 *Journal of Digital Earth*, 16(2):4668–4686, 2023.

600 Xiayin Lou, Peng Luo, Ziqi Li, Song Gao, and Liqiu Meng. Geoxcp: uncertainty quantification of  
 601 spatial explanations in explainable ai. *International Journal of Geographical Information Science*,  
 602 pp. 1–31, 2025a.

603

604 Xiayin Lou, Peng Luo, and Liqiu Meng. Geoconformal prediction: a model-agnostic framework for  
 605 measuring the uncertainty of spatial prediction. *Annals of the American Association of Geogra-  
 606 phers*, pp. 1–28, 2025b.

607 Chris Lu, Samuel Holt, Claudio Fanconi, Alex Chan, Jakob Foerster, Mihaela van der Schaar, and  
 608 Robert Lange. Discovering preference optimization algorithms with and for large language mod-  
 609 els. *Advances in Neural Information Processing Systems*, 37:86528–86573, 2024.

610 Peng Luo, Yongze Song, Di Zhu, Junyi Cheng, and Liqiu Meng. A generalized heterogeneity model  
 611 for spatial interpolation. *International Journal of Geographical Information Science*, 37(3):634–  
 612 659, 2023.

613

614 Peng Luo, Yilong Wu, and Yongze Song. Feature-free regression kriging. *arXiv preprint*  
 615 *arXiv:2507.07382*, 2025.

616 Yecheng Jason Ma, William Liang, Guanzhi Wang, De-An Huang, Osbert Bastani, Dinesh Jayara-  
 617 man, Yuke Zhu, Linxi Fan, and Anima Anandkumar. Eureka: Human-level reward design via  
 618 coding large language models, 2024. URL <https://arxiv.org/abs/2310.12931>.

619

620 Gengchen Mai, Weiming Huang, Jin Sun, Suhang Song, Deepak Mishra, Ninghao Liu, Song Gao,  
 621 Tianming Liu, Gao Cong, Yingjie Hu, et al. On the opportunities and challenges of foundation  
 622 models for geospatial artificial intelligence. *arXiv preprint arXiv:2304.06798*, 2023.

623 Harvey J Miller. Tobler’s first law and spatial analysis. *Annals of the association of American*  
 624 *geographers*, 94(2):284–289, 2004.

625

626 Clint Morris, Michael Jurado, and Jason Zutty. Llm guided evolution-the automation of models  
 627 advancing models. In *Proceedings of the Genetic and Evolutionary Computation Conference*, pp.  
 628 377–384, 2024.

629

630 Alexander Novikov, Ng n V , Marvin Eisenberger, Emilien Dupont, Po-Sen Huang, Adam Zsolt  
 631 Wagner, Sergey Shirobokov, Borislav Kozlovskii, Francisco JR Ruiz, Abbas Mehrabian,  
 632 et al. Alphaevolve: A coding agent for scientific and algorithmic discovery. *arXiv preprint*  
*arXiv:2506.13131*, 2025.

633

634 Chen Qian, Wei Liu, Hongzhang Liu, Nuo Chen, Yufan Dang, Jiahao Li, Cheng Yang, Weize Chen,  
 635 Yusheng Su, Xin Cong, et al. Chatdev: Communicative agents for software development, 2024.  
 636 URL <https://arxiv.org/abs/2307.7924>, 2024.

637

638 Zackary Rackauckas. Rag-fusion: a new take on retrieval-augmented generation. *arXiv preprint*  
*arXiv:2402.03367*, 2024.

639

640 Bernardino Romera-Paredes, Mohammadamin Barekatain, Alexander Novikov, Matej Balog,  
 641 M Pawan Kumar, Emilien Dupont, Francisco JR Ruiz, Jordan S Ellenberg, Pengming Wang,  
 642 Omar Fawzi, et al. Mathematical discoveries from program search with large language models.  
*Nature*, 625(7995):468–475, 2024.

643

644 Asankhaya Sharma. Openevolve: an open-source evolutionary coding agent, 2025. URL <https://github.com/codelion/openevolve>.

645

646 Anja Surina, Amin Mansouri, Lars Quaedvlieg, Amal Seddas, Maryna Viazovska, Emmanuel Abbe,  
 647 and Caglar Gulcehre. Algorithm discovery with llms: Evolutionary search meets reinforcement  
 learning. *arXiv preprint arXiv:2504.05108*, 2025.

648 Petar Veličković, Alex Vitvitskyi, Larisa Markeeva, Borja Ibarz, Lars Buesing, Matej Balog, and  
 649 Alexander Novikov. Amplifying human performance in combinatorial competitive programming.  
 650 *arXiv preprint arXiv:2411.19744*, 2024.

651  
 652 Lei Wang, Chen Ma, Xueyang Feng, Zeyu Zhang, Hao Yang, Jingsen Zhang, Zhiyuan Chen, Jiakai  
 653 Tang, Xu Chen, Yankai Lin, et al. A survey on large language model based autonomous agents.  
 654 *Frontiers of Computer Science*, 18(6):186345, 2024.

655 Guangzhi Xiong, Eric Xie, Amir Hassan Shariatmadari, Sikun Guo, Stefan Bekiranov, and Aidong  
 656 Zhang. Improving scientific hypothesis generation with knowledge grounded large language mod-  
 657 els. *arXiv preprint arXiv:2411.02382*, 2024.

658 Dazhou Yu, Riyang Bao, Gengchen Mai, and Liang Zhao. Spatial-rag: Spatial retrieval augmented  
 659 generation for real-world spatial reasoning questions. *arXiv preprint arXiv:2502.18470*, 2025.

660  
 661 Zhilun Zhou, Yuming Lin, Depeng Jin, and Yong Li. Large language model for participatory urban  
 662 planning. *arXiv preprint arXiv:2402.17161*, 2024.

## 664 A APPENDIX

### 666 A.1 SPATIAL REGRESSION MODEL

668 **Task- Spatial regression** Spatial regression explicitly introduces geospatial context into the sta-  
 669 tistical framework of regression. One wants to combine space with the statistical models when he  
 670 or she thinks geospatial space can play an essential role in the data generation process or use space  
 671 as a proxy for some factors difficult to obtain.

672 **Model- GWR** In this work, we selected geographically weighted regression (GWR) (Fothering-  
 673 ham et al., 2009), one of the most famous spatial regression models. For GWR, the regression  
 674 coefficients are not fixed, but depend on the geographical coordinates of observations, which is  
 675 defined as follows:

$$677 \quad y_i = \beta_0(u_i, v_i) + \sum_{k=1}^K \beta_k(u_i, v_i)x_{ik} + \varepsilon \quad (3)$$

679 where  $(u_i, v_i)$  are the geographical coordinates.

681 **Evaluator** As for GWR, we use the coefficient of determination ( $R^2$ ) as the evaluation metric.  
 682 Our objective is to obtain an evolved GWR model that has the highest  $R^2$ .

684 **Datasets** The Georgia census data<sup>2</sup> is extracted from GWmodel, a R package that contains a group  
 685 of geographically weighted models. The original data contains 7 variables and 2 pairs of geograph-  
 686 ical coordinates expressed in geodetic and projected coordinate systems, respectively. In this work,  
 687 we employ the percentage of the county population with a bachelor’s degree as the target variable,  
 688 and the other 6 variables (total population, rural population percentage, elderly (65+) population per-  
 689 centage, foreign-born population percentage, population living below the poverty line percentage,  
 690 black population percentage) as explanatory variables.

### 692 A.2 USE OF LLMs

693 We use LLMs to polish selected paragraphs and to automatically extract differences between algo-  
 694 rithms (e.g., Kriging and GeoCP) produced by different code-generation methods (e.g., OpenEvolve  
 695 and GeoEvolve), thereby facilitating the analysis of GeoEvolve’s specific improvements and their  
 696 underlying causes. All research ideas were independently conceived by the authors.

### 698 A.3 CODE ANALYZER

700 Figure 6 shows the template of the Code Analyzer and an example output.

701<sup>2</sup><https://r-packages.io/datasets/Georgia>

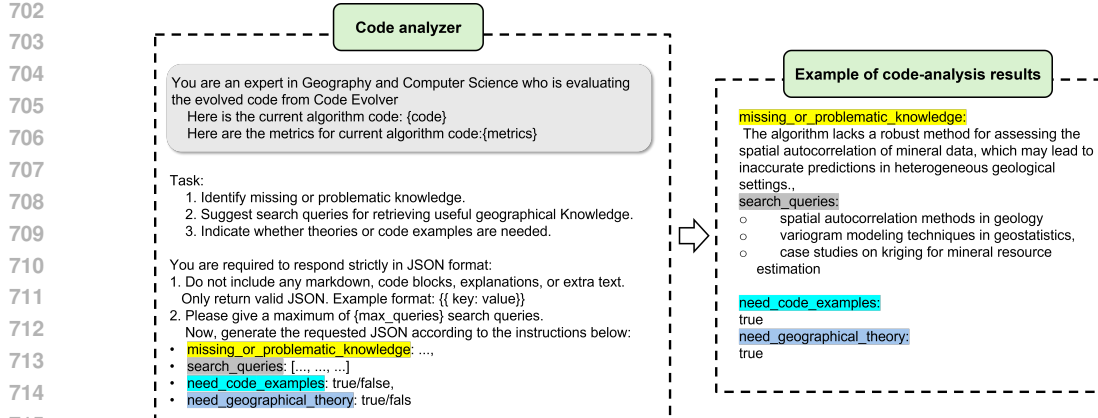


Figure 6: The template and an example of code analyzer

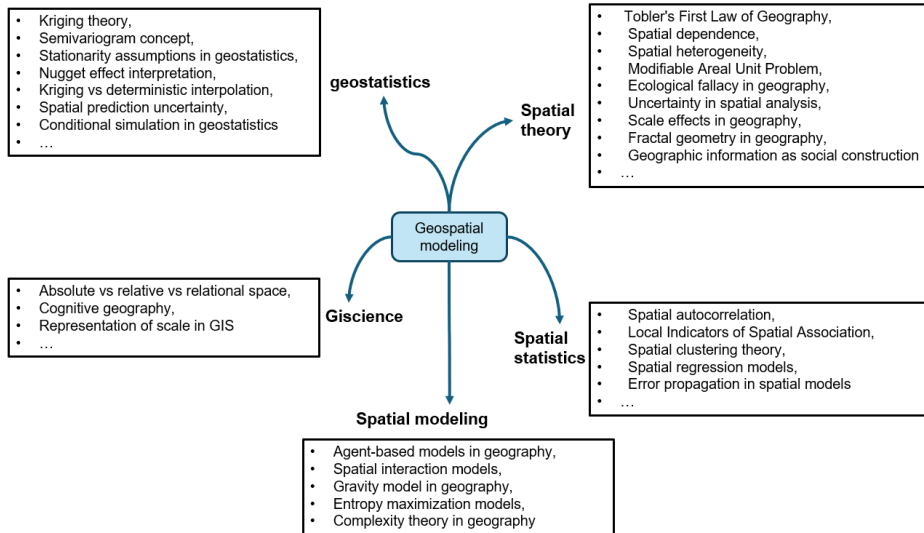


Figure 7: The keywords used for constructing geospatial knowledge database

#### A.4 GEOSPATIAL KNOWLEDGE DATABASE

The geospatial knowledge is initialized automatically from web (e.g., arxiv, wikipedia, github, etc.) according to the user-defined keywords and can be updated according to the requirements dynamically during evolution. Figure 7 shows an example of constructed geospatial knowledge database, the five categories are geostatistics, spatial theory, GIScience, spatial statistics, and spatial modeling.

It should be noted that the construction of a geospatial knowledge base can include many more keywords, enabling a much larger scale—potentially comprising thousands of documents or developed through more sophisticated processes. In the present experiments, however, we intentionally created a small-scale knowledge base to validate the effectiveness of GeoEvolve on three algorithmic tasks. We expect that GeoEvolve will achieve even greater performance gains when combined with a larger and more comprehensive geospatial knowledge base in future work.

#### A.5 BENCHMARK METHODS

Figure 8 illustrates the GeoEvolve without RAG version used in our ablation study. The algorithm still consists of an outer loop and an inner loop. After the agent proposes an improvement to the algorithm in the inner loop, the code analyzer evaluates the updated code. In this version, the system

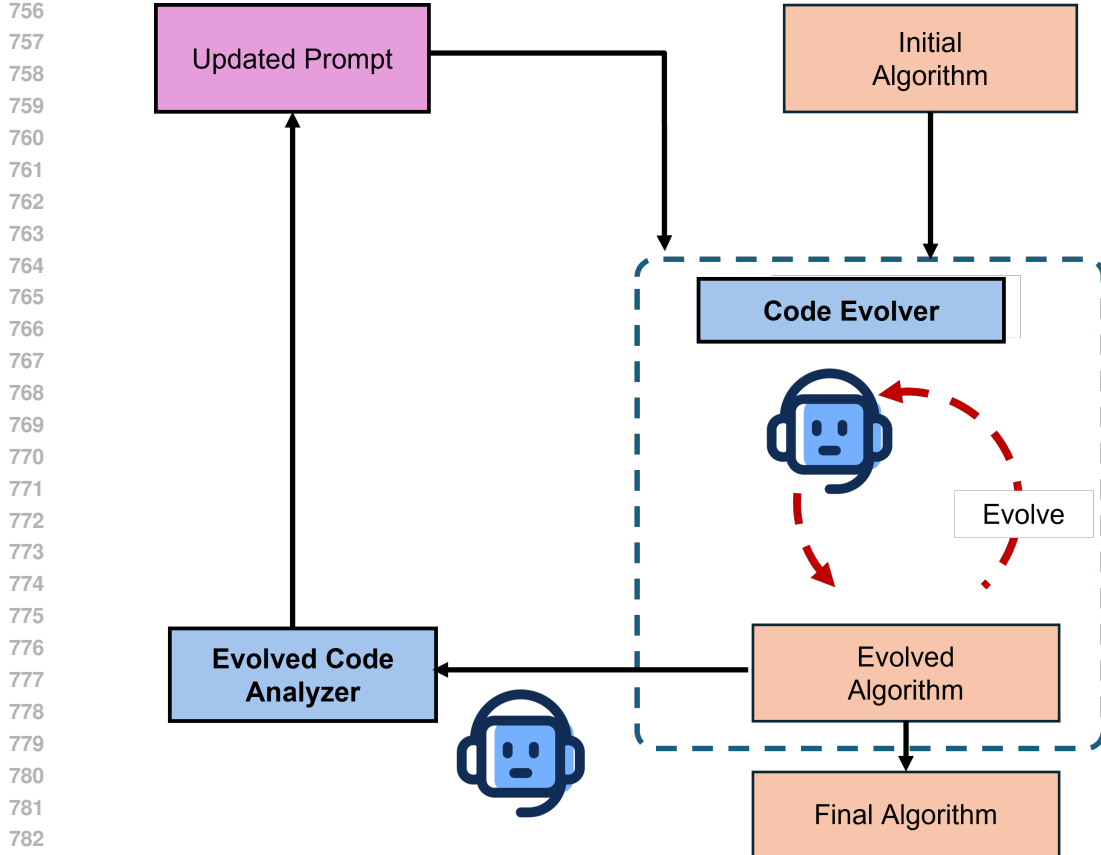


Figure 8: GeoEvolve without RAG

does not retrieve any information from the GeoKnowRAG geospatial knowledge base; instead, it directly updates the prompt and returns to the inner loop to further evolve the algorithm.

#### A.6 LLM CONFIGURATION

To ensure reproducibility and a fair comparison across model families, we report the exact large language models (LLMs) used in all components of our system, including the OpenEvolve baseline, the GeoEvolve framework, the GeoKnowRAG retrieval module, and the outer-loop agentic controller. Across all LLM families (GPT, Gemini, Qwen), we adopt a consistent two-tier strategy: a *primary* model for code mutation and generation, and a *secondary* model for validation, refinement, and fallback reasoning. Retrieval modules use the corresponding embedding model for vectorization, and the agent controller employs a lightweight but reasoning-capable model to support outer-loop decision making.

**GPT family.** OpenEvolve uses GPT-4o as the primary evolver and GPT-4.1 as the secondary validator. GeoEvolve adopts the same configuration. GeoKnowRAG embeds all knowledge documents using text-embedding-3-large. The outer-loop agent controller also operates on GPT-4.1, balancing reasoning depth and runtime efficiency.

**Gemini family.** Both OpenEvolve and GeoEvolve use Gemini-2.5-flash as the primary evolver and Gemini-2.5-pro as the secondary model. GeoKnowRAG employs gemini-embedding-001, and the agent controller runs on Gemini-2.5-flash.

**Qwen family.** For the Qwen models, OpenEvolve and GeoEvolve use Qwen3-235B (primary) and Qwen3-32B (secondary). GeoKnowRAG uses qwen3-embedding-8B, and the agent controller also runs on Qwen3-32B.

810  
811  
Table 3: LLM configuration for all components of OpenEvolve and GeoEvolve.  
812  
813

Component	GPT	Gemini	Qwen
OpenEvolve (primary)	GPT-4o	Gemini-2.5-flash	Qwen3-235B
OpenEvolve (secondary)	GPT-4.1	Gemini-2.5-pro	Qwen3-32B
GeoEvolve (primary)	GPT-4o	Gemini-2.5-flash	Qwen3-235B
GeoEvolve (secondary)	GPT-4.1	Gemini-2.5-pro	Qwen3-32B
GeoKnowRAG embeddings	text-embedding-3-large	gemini-embedding-001	qwen3-embedding-8B
Agent controller	GPT-4.1	Gemini-2.5-flash	Qwen3-32B

814  
815  
816  
817  
818  
Table 4: Runtime comparison of GeoEvolve and OpenEvolve variants using GPT-4.1 across three  
819  
820  
821  
geospatial tasks.  
822  
823

RAG Setting	Task	Dataset	Time (s)	Hours
GeoEvolve (Dynamic RAG)	Kriging	Australia Minerals	3085.37	0.86
	GeoCP	Seattle House Price	4546.91	1.26
	GWR	Georgia Census	1862.72	0.52
GeoEvolve (Static RAG)	Kriging	Australia Minerals	2730.55	0.76
	GeoCP	Seattle House Price	4750.32	1.32
	GWR	Georgia Census	2446.12	0.68
GeoEvolve (No RAG)	Kriging	Australia Minerals	2065.91	0.57
	GeoCP	Seattle House Price	2235.45	0.62
	GWR	Georgia Census	1786.66	0.50
OpenEvolve (No GeoKnowledge)	Kriging	Australia Minerals	1192.98	0.33
	GeoCP	Seattle House Price	402.89	0.15
	GWR	Georgia Census	343.55	0.10
OpenEvolve (General GeoKnowledge)	Kriging	Australia Minerals	1670.90	0.46
	GeoCP	Seattle House Price	380.93	0.11
	GWR	Georgia Census	100.61	0.03
OpenEvolve (Specific GeoKnowledge)	Kriging	Australia Minerals	1437.91	0.40
	GeoCP	Seattle House Price	539.68	0.15
	GWR	Georgia Census	667.19	0.19

824  
825  
826  
827  
828  
829  
830  
831  
832  
833  
834  
835  
836  
837  
838  
839  
This unified LLM configuration is crucial for interpreting our ablations. The GeoEvolve without  
840  
GeoKnowRAG variant keeps the *identical* primary and secondary models, ensuring that per-  
841  
formance differences arise solely from the absence of structured domain knowledge rather than changes  
842  
in model capacity. Similarly, using matched primary/secondary pairs across OpenEvolve and Geo-  
843  
Evolve removes confounding effects from heterogeneous model dependencies. In our experiments,  
844  
replacing the secondary models with weaker reasoning engines leads to noticeably less stable evo-  
845  
lutionary trajectories, confirming that fallback validation is essential for preventing code drift and  
846  
maintaining interpretable improvements. Thus, the LLM design is not merely an implementation  
847  
detail but a controlled experimental factor that enables clean causal attribution in our ablation study.  
848849  
850  
A.7 TIME851  
852  
853  
854  
855  
856  
857  
858  
859  
860  
861  
Table 4 reports the full runtime comparison of GeoEvolve and OpenEvolve using GPT-4.1 across  
862  
the three geospatial tasks. Overall, GeoEvolve incurs additional computational cost due to its two-  
863  
level agentic control loop and the GeoKnowRAG retrieval mechanism, but the overhead is consistent  
864  
and interpretable. For Dynamic RAG, GeoEvolve requires 0.52–1.26 hours per task, while Static  
865  
RAG slightly reduces the overhead to 0.68–1.32 hours. Removing RAG reduces the runtime further  
866  
to 0.50–0.62 hours, confirming that a substantial portion of the overhead comes from knowledge  
867  
retrieval rather than code evolution itself. In contrast, OpenEvolve—without geospatial knowledge  
868  
integration—runs considerably faster (0.03–0.33 hours), but this speed comes at the cost of weaker  
869  
algorithmic improvements. These results reflect a clear trade-off: integrating structured geospatial  
870  
knowledge increases runtime but enables GeoEvolve to produce substantially stronger and more  
871  
stable algorithmic improvements.872  
873  
Figure 9 presents the average runtime of GeoEvolve across three LLM families (GPT-4.1, Gemini-  
874  
2.5, and Qwen3-32B) under both Dynamic and Static RAG settings. Two clear patterns emerge from  
875  
the results.

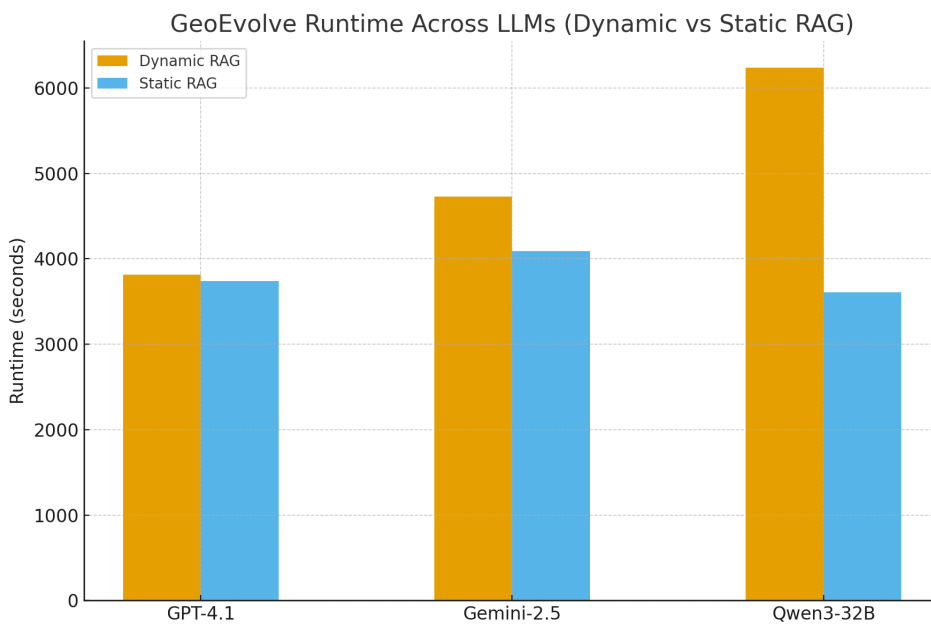


Figure 9: Average runtime of GeoEvolve across three LLM families (GPT-4.1, Gemini-2.5, and Qwen3-32B) under Dynamic and Static RAG.

First, the choice of LLM strongly affects computational cost. GPT-4.1 achieves the lowest runtime (approximately 3.7k seconds), Gemini-2.5 is moderately slower (around 4.1–4.7k seconds), and Qwen3-32B is the slowest (over 6.2k seconds). This ordering reflects the inherent inference latency of each model, indicating that GeoEvolve’s execution time scales proportionally with the underlying LLM’s response speed.

Second, Static RAG consistently outperforms Dynamic RAG in runtime across all LLMs. Static RAG avoids repeated retrieval–summarization cycles in the outer loop, whereas Dynamic RAG regenerates the knowledge context at every iteration, leading to additional overhead. The effect is particularly pronounced for Qwen3-32B, where Dynamic RAG incurs nearly 70% more latency compared with Static RAG.

Overall, these results highlight a practical trade-off: Dynamic RAG provides higher retrieval adaptivity at the cost of increased runtime, while Static RAG offers more efficient execution with slightly reduced flexibility. This confirms that (i) geospatial algorithm evolution is sensitive to LLM inference speed, and (ii) users may balance computational efficiency and retrieval precision by choosing between Static and Dynamic RAG modes.

#### A.8 GENERALIZATION EXPERIMENT

##### A.8.1 DATASETS

We selected 3 datasets per task (9 total datasets) to ensure comprehensive coverage.

- Kriging: Australian Minerals, Ocean Chlorophyll, Temperature Station Data.
- GeoCP: Seattle Housing Price, US Life Expectancy, China PM2.5.
- GWR (New): Georgia Education, NYC Income, Chicago Health.

The detailed descriptions about the datasets used in this work is displayed in Table 5.

##### A.8.2 DOMAIN GENERALIZATION

Our goal is to demonstrate robust cross-domain transferability. We expect the models evolved on a source domain (e.g., housing prices) to effectively generalize to target domains (e.g., minerals).

Model	Name	Description
Kriging	Australian Minerals	Spatial measurements of Cu, Pb, and Zn from a region in Australia, selected for their significance as indicators of environmental contamination and ecological health.
Kriging	Ocean Chlorophyll	The Ocean Chlorophyll dataset includes 4,136 highly clustered chlorophyll observations collected near Townsville, Australia.
Kriging	Temperature Station Data	90-day ambient temperature covering Los Angeles County from 1st January to 31st March, 2019, collected from Weather Underground.
GeoCP	Seattle Housing	Home sales prices and characteristics for Seattle.
GeoCP	US Life Expectancy	Life expectancy and related sociodemographic variables for US counties.
GeoCP	China PM2.5	PM2.5 concentration and related variables for China cities
GWR	Georgia Education	Census data about education from the county of Georgia, USA
GWR	NYC Income	Block-level Earnings New York City (2002-14) from Longitudinal Employer-Household Dynamics (LEHD).
GWR	Chicago Health	Public health and socio-economic indicators for the 77 community areas of Chicago, IL, 2014.

Table 5: Details about datasets employed in the domain generalization experiment

Specifically, the evolution phase was conducted on the Australian Minerals dataset for Kriging, Seattle Housing for GeoCP, and Georgia Education for GWR. The results for three models are as follows.

**Kriging** Kriging Task (RMSE  $\downarrow$ ): OpenEvolve baselines exhibit catastrophic failure (divergence) on the Ocean Chlorophyll dataset, whereas GeoEvolve remains robust (see Table 6).

Table 6: Model performance comparison of evolved Kriging

Model	Australian Minerals			Ocean	Temperature
	Cu	Pb	Zn	Chlorophyll	
Original	0.9139	0.6619	0.6294	0.9949	1.1567
GeoEvolve (Dynamic RAG)	0.8718	0.6131	<b>0.5852</b>	0.9916	1.1634
GeoEvolve (Static RAG)	<b>0.8602</b>	<b>0.5927</b>	0.5941	0.6179	<b>0.5417</b>
GeoEvolve (No RAG)	<b>0.8602</b>	<b>0.5927</b>	0.5941	<b>0.5441</b>	1.0499
OpenEvolve (No GeoKnow)	0.8727	0.6413	0.6245	<b>0.5296</b>	1.1083
OpenEvolve (General GeoKnow)	0.9264	0.6519	0.6333	0.6158	2.0221
OpenEvolve (Specific GeoKnow)	0.9139	0.6632	0.6338	Fail (460.4035)	5.7484

**GeoCP** GeoCP Task (Interval Score  $\downarrow$ ): Dynamic RAG achieves the best scores across all datasets, significantly reducing uncertainty compared to baselines (see Table 7).

**GWR** GWR Task ( $R^2 \uparrow$ ): GeoEvolve (Dynamic RAG) consistently achieves the highest or near-highest  $R^2$ , demonstrating strong transferability. In contrast, OpenEvolve with Specific GeoKnow performs poorly on the source domain (Georgia), indicating overfitting or prompt misalignment (see Figure 8).

Table 7: Model performance comparison of evolved GeoCP

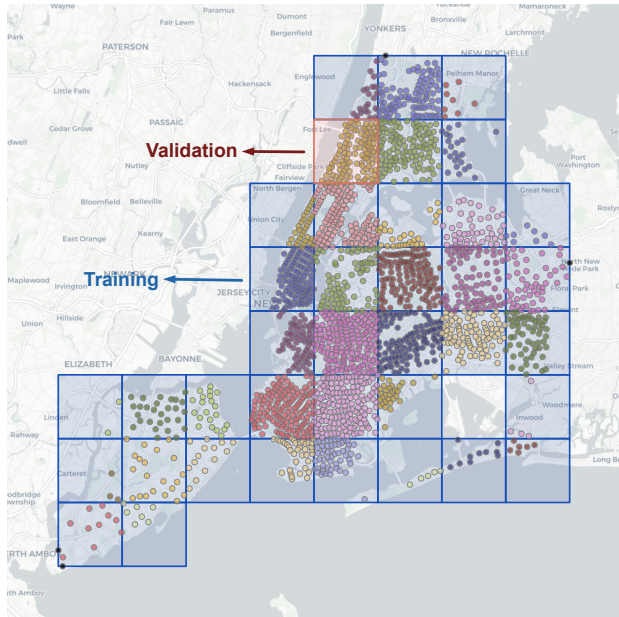
Model	Dataset	Interval Score ↓	Coverage	Avg Interval Size
Original	Seattle House Price	44.7611	0.9533	18.3254
	US Life Expectancy	121.4673	0.9098	50.2762
	China PM2.5	23.4409	0.9295	10.6332
GeoEvolve (Dynamic RAG)	Seattle House Price	<b>41.2389</b>	0.9000	13.7750
	US Life Expectancy	<b>113.2176</b>	0.8922	41.5560
	China PM2.5	<b>21.0186</b>	0.9507	9.3529
GeoEvolve (Static RAG)	Seattle House Price	45.2738	0.9600	18.7862
	US Life Expectancy	123.5681	0.9424	53.4537
	China PM2.5	<b>21.0186</b>	0.9507	9.3529
GeoEvolve (No RAG)	Seattle House Price	44.2545	0.9433	17.5586
	US Life Expectancy	141.2780	0.9424	67.3331
	China PM2.5	24.0525	0.9437	10.9554
OpenEvolve (No GeoKnow)	Seattle House Price	43.1823	0.9333	16.9139
	US Life Expectancy	123.4440	0.8897	45.9977
	China PM2.5	26.1946	0.9146	9.4270
OpenEvolve (General GeoKnow)	Seattle House Price	42.8343	0.9333	17.1508
	US Life Expectancy	124.3828	0.9023	51.4155
	China PM2.5	27.0417	0.9085	10.0772
OpenEvolve (Specific GeoKnow)	Seattle House Price	41.4267	0.9033	13.9557
	US Life Expectancy	124.0236	0.8671	42.2759
	China PM2.5	26.7654	0.8732	8.1674

Table 8: Model performance comparison of evolved GWR

Model	Georgia Education	NYC Income	Chicago Health
Original	0.1564	0.7065	0.5999
GeoEvolve (Dynamic RAG)	0.3556	<b>0.7385</b>	<b>0.6221</b>
GeoEvolve (Static RAG)	<b>0.4524</b>	0.5039	0.4927
GeoEvolve (No RAG)	<b>0.4524</b>	0.5038	0.5388
OpenEvolve (No GeoKnow)	0.2287	0.6238	0.5388
OpenEvolve (General GeoKnow)	0.2353	0.6317	0.6008
OpenEvolve (Specific GeoKnow)	0.1367	0.7297	0.6074

1026 A.8.3 SPATIAL GENERALIZATION  
1027

1028 For geospatial models, spatial generalization is equally important. Taking GWR for New York  
1029 income dataset as an example, we use a Spatial Leave-One-Out (SpatialLOO) approach (training on  
1030  $N - 1$  regions, testing on held-out region). Figure 10 offers a general illustration of SpatialLOO.  
1031 GeoEvolve with Dynamic RAG achieved the lowest RMSE and standard deviation, proving it adapts  
1032 best to unseen spatial distributions. The performance of spatial generalization is shown in the Table  
1033 9.

1055 Figure 10: Spatial Leave-One-Out sampling for evaluating spatial generalization  
10561057  
1058 Table 9: Performance of spatial generalization  
1059

Model	Mean RMSE	Std RMSE
Original	2.165	1.66
GeoEvolve with Dynamic RAG	<b>1.968</b> ↓	<b>1.532</b> ↓
GeoEvolve with Static RAG	2.3 ↑	1.571 ↓
GeoEvolve without RAG	2.289 ↑	1.687 ↑
OpenEvolve without GeoKnow	2.432 ↑	1.707 ↑
OpenEvolve with General GeoKnow	2.059 ↑	1.641 ↑
OpenEvolve with Specific GeoKnow	2.378 ↑	2.366 ↑

1071 A.8.4 TEMPORAL GENERALIZATION  
1072

1073 Temporal generalization can also be vital in tasks involving spatiotemporal prediction, so we design  
1074 experiments for evaluating temporal generalization performance: ensuring that a geospatial model  
1075 evolved on data from one specific time period (e.g., 2024) maintains high performance when applied  
1076 to datasets from a different time period (e.g., 2025).

1077 Taking Kriging for temperature interpolation as an example, we trained on historical data (Jan 2019)  
1078 and tested on future data (next 100 days). As shown in Table 10, GeoEvolve with Static RAG yielded  
1079 the highest mean improvement (0.39), while OpenEvolve variants caused performance degradation  
(negative improvement).

Table 10: Performance of temporal generalization

Model	Avg. Improvement	Med. Improvement	Std	Min	Max
GeoEvolve with Dynamic RAG	-0.00325	-0.00312	0.00125	-0.00698	0.00012
GeoEvolve with Static RAG	<b>0.39243</b>	<b>0.44375</b>	0.22398	-0.40564	0.71676
GeoEvolve without RAG	0.05269	0.05169	0.02014	-0.00796	0.10649
OpenEvolve with General GeoKnow	-0.38191	-0.33568	0.17768	-0.86385	-0.16534
OpenEvolve with Specific GeoKnow	-3.02455	-2.93563	0.75308	-4.49663	-1.75598
OpenEvolve without GeoKnow	0.02625	0.01741	0.03027	-0.01006	0.12728

### A.9 ORIGINAL ALGORITHM

#### A.9.1 ORIGINAL ALGORITHM OF ORIDINARY KRIGING.

Kriging is a geostatistical spatial interpolation method that provides the *best linear unbiased estimator* (BLUE) of an unknown value at a location by optimally weighting surrounding observations. It assumes that the spatial process  $Z(s)$  can be represented as

$$Z(s) = \mu + \varepsilon(s), \quad (4)$$

where  $\mu$  is an unknown constant mean and  $\varepsilon(s)$  is a zero-mean, second-order stationary random field. The key assumption of second-order stationarity requires that the mean is constant and that the covariance depends only on the lag vector  $h$ , i.e.,

$$\text{Cov} [Z(s), Z(s + h)] = C(h), \quad (5)$$

or equivalently through the semivariogram  $\gamma(h)$ .

Ordinary kriging predicts the value at an unsampled location  $s_0$  as a weighted linear combination of the observed data:

$$\hat{Z}(s_0) = \sum_{i=1}^n \lambda_i Z(s_i), \quad (6)$$

subject to the unbiasedness constraint

$$\sum_{i=1}^n \lambda_i = 1. \quad (7)$$

The kriging weights  $\lambda_i$  are determined by minimizing the estimation variance

$$\sigma_k^2 = \text{Var} [\hat{Z}(s_0) - Z(s_0)] \quad (8)$$

using the spatial covariance or variogram model.

#### A.9.2 ORIGINAL ALGORITHM OF GEOCP

GeoConformal Prediction (GeoCP) is a model-agnostic framework for quantifying spatial prediction uncertainty by extending *conformal prediction* (CP) with explicit geographic weighting. Conformal prediction provides finite-sample, distribution-free prediction intervals by computing nonconformity scores on a calibration set and selecting the  $(1 - \varepsilon)$  quantile to guarantee coverage. However, standard CP assumes data exchangeability and yields intervals of constant width, which is violated in geospatial settings where strong spatial heterogeneity and covariate shift are common.

To overcome these limitations, GeoCP integrates spatial dependence directly into the conformal framework. Given a geospatial model  $f : \mathcal{X} \rightarrow \mathcal{Y}$  trained on a set of observations and a calibration set  $\{(X_i, y_i)\}_{i=1}^m$ , let  $a(\cdot)$  be a nonconformity score (e.g., absolute residual) and  $a_i = a(f(X_i), y_i)$  for calibration point  $i$ . For a test location  $X_{\text{test}}$  with geographic coordinates  $(u_{\text{test}}, v_{\text{test}})$ , GeoCP assigns each calibration point  $i$  a geographic weight

$$w_i(u_{\text{test}}, v_{\text{test}}) = \frac{K_\sigma(d((u_{\text{test}}, v_{\text{test}}), (u_i, v_i)))}{\sum_{j=1}^m K_\sigma(d((u_{\text{test}}, v_{\text{test}}), (u_j, v_j)))}, \quad (9)$$

where  $d(\cdot, \cdot)$  is the geographic distance and  $K_\sigma$  is a distance-decay kernel (e.g., Gaussian). These weights reflect Tobler’s first law of geography—that nearby observations are more similar—thus relaxing the exchangeability requirement of classical CP.

1134 The GeoCP prediction interval for  $X_{\text{test}}$  is then defined as  
 1135

$$1136 C_{\text{geo}}(X_{\text{test}}) = \{y : a(f(X_{\text{test}}), y) \leq Q_{1-\varepsilon}^{\text{geo}}(\{a_i\}, \{w_i(u_{\text{test}}, v_{\text{test}})\})\}, \quad (10)$$

1137 where  $Q_{1-\varepsilon}^{\text{geo}}$  is the geographically weighted  $(1 - \varepsilon)$ -quantile computed as  
 1138

$$1139 Q_{1-\varepsilon}^{\text{geo}} = \inf \left\{ q : \sum_{i=1}^m w_i(u_{\text{test}}, v_{\text{test}}) \mathbf{1}\{a_i \leq q\} \geq 1 - \varepsilon \right\}. \quad (11)$$

1142 Algorithmically, GeoCP proceeds as follows: (1) split the dataset into training, calibration, and test  
 1143 sets; (2) fit the spatial prediction model  $f$  on the training set; (3) compute nonconformity scores  $\{a_i\}$   
 1144 on the calibration set; (4) for each test point, calculate geographic weights  $w_i$  via (9); (5) determine  
 1145 the geographically weighted quantile (11) and form the prediction interval (10).  
 1146

1147 By construction, GeoCP inherits the rigorous finite-sample coverage guarantee of conformal predic-  
 1148 tion,

$$1149 \mathbb{P}[y_{\text{test}} \in C_{\text{geo}}(X_{\text{test}})] \geq 1 - \varepsilon,$$

1150 while producing *spatially varying* prediction intervals that directly reflect local heterogeneity. Be-  
 1151 cause it does not require modifying the underlying predictive model, GeoCP can be applied seam-  
 1152 lessly to classical geostatistical methods (e.g., Kriging) and modern GeoAI models, providing a  
 1153 unified and interpretable framework for uncertainty quantification and supporting fair, responsible  
 1154 geographic decision-making.

## 1155 A.10 EVOLVED KRIGING MODEL

### 1156 A.10.1 GEOEVOLVE-KRIGING (OUR MODEL)

1159 Compared with the original Ordinary Kriging, GeoEvolve–Kriging preserves the core structure  
 1160 while introducing the following key innovations:

- 1162 • **Expanded and automatically selected variogram family.** Instead of a single non-  
 1163 standard exponential model, GeoEvolve fits a flexible family

$$1164 \gamma_{\theta}(h) = \theta_0 + \theta_1 \left[ 1 - \exp(-(h/\theta_2)^p) \right], \quad (12)$$

1166 where  $p = 1$  yields the exponential model,  $p = 2$  the Gaussian model,  
 1167 and  $p \in (0, 2)$  the Matérn family (with smoothness  $\nu$ ). Candidate models  
 1168  $\{\text{Exponential, Gaussian, Linear, Matérn}\}$  are compared using information criteria such as  
 1169

$$1170 \text{AIC} = 2k - 2 \log L, \quad \text{BIC} = k \log n - 2 \log L, \quad (13)$$

1171 and the optimal variogram is selected by minimum AIC/BIC. This multi-model, multi-start  
 1172 search avoids local minima and captures a wide spectrum of spatial smoothness.

- 1173 • **Adaptive empirical variogram estimation.** GeoEvolve constructs the empirical semi-  
 1174 variogram using adaptive binning based on Silverman’s rule or quantiles:

$$1176 \hat{\gamma}(h_k) = \frac{1}{2|N(h_k)|} \sum_{(i,j) \in N(h_k)} [Z(x_i) - Z(x_j)]^2, \quad (14)$$

1178 where  $N(h_k)$  is the set of pairs with distances in the  $k$ th adaptive bin. Robust trimmed  
 1179 means and an automatic choice of  $n_{\text{lags}} \in [8, 20] \propto \sqrt{n}$  reduce the impact of outliers and  
 1180 distance heterogeneity.

- 1182 • **Robust model fitting.** Parameter estimation in (12) is performed via multi-start global  
 1183 optimization with either

$$1184 \min_{\theta} \sum_k w_k |\hat{\gamma}(h_k) - \gamma_{\theta}(h_k)| \quad (15)$$

1186 (robust L1 loss) or weighted least squares, depending on empirical residual patterns, where  
 1187  $w_k$  are bin-based weights. This strategy guards against local minima and ensures sill  $\theta_1$   
 1188 and range  $\theta_2$  remain physically meaningful.

1188  
 1189  
 1190  
 1191  
 1192  
 1193  
 1194  
 1195  
 1196  
 1197  
 1198  
 1199  
 1200  
 1201  
 1202  
 1203  
 1204  
 1205  
 1206  
 1207  
 1208  
 1209  
 1210  
 1211  
 1212  
 1213  
 1214  
 1215  
 1216  
 1217  
 1218  
 1219  
 1220  
 1221  
 1222  
 1223  
 1224  
 1225  
 1226  
 1227  
 1228  
 1229  
 1230  
 1231  
 1232  
 1233  
 1234  
 1235  
 1236  
 1237  
 1238  
 1239  
 1240  
 1241

- **Localized kriging with adaptive regularization.** To improve scalability and stability, GeoEvolve restricts the kriging system to the  $K$  nearest neighbors (e.g.,  $K = 25$ ) of  $x_0$  using a cKDTree and adds a condition-number-dependent diagonal adjustment:

$$\mathbf{K}_{\text{loc}}\lambda = \mathbf{k}_{\text{loc}}, \quad \mathbf{K}_{\text{loc}} \leftarrow \mathbf{K}_{\text{loc}} + \epsilon(\kappa)\mathbf{I}, \quad (16)$$

where  $\epsilon(\kappa)$  is an adaptive nugget (e.g.,  $10^{-10}$  to  $10^{-4}$ ) determined by the matrix condition number  $\kappa$ . This reduces computational cost from  $O(n^3)$  to  $O(K^3)$  and stabilizes inversion in ill-conditioned settings.

- **Adaptive data transformation.** GeoEvolve applies an adaptive log transform

$$Z' = \log(Z + \delta), \quad (17)$$

where the offset  $\delta$  is chosen from the 1st percentile of positive values plus a small  $\epsilon$  to reduce skewness and ensure valid back-transformation.

### A.10.2 COMPARISON OF EVOLVED KRIGING FROM DIFFERENT MODELS

In this section, we analyze the main technical components of different algorithm:

**Variogram family.** Original uses only the exponential variogram with a non-standard form  $nugget + sill(1 - e^{-h/range})$ . OpenEvolve standardizes the form to  $e^{-h/range}$  and adds Gaussian and Linear options. OpenEvolve with GeoKnowledge adopts the same set but applies automatic model selection among candidate models. GeoEvolve further introduces the Matern family ( $\nu = 0.2\text{--}3.0$ ) with full AIC/BIC-based automatic selection and multi-start optimization.

**Empirical variogram.** Original employs 12 equal-width bins including zero distance and is unweighted. OpenEvolve truncates distances to 85% of the maximum and removes NaN bins. OpenEvolve with GeoKnowledge follows the same procedure but adds minimal pair control. GeoEvolve uses adaptive binning via Silverman's rule or quantiles, applies a robust trimmed mean, and automatically sets  $n_{\text{lags}} = 8\text{--}20 \propto \sqrt{n}$ .

**Model fitting.** Original applies an L1 loss with a single L-BFGS-B run. OpenEvolve still uses L1 but adds parameter bounds, smart initialization, and a fallback strategy. OpenEvolve with GeoKnowledge switches to L2 loss and selects the best model by minimum MSE. GeoEvolve adopts a robust L1 loss, multi-start global search, Matern smoothness grid, and AIC/BIC complexity penalties.

**Kriging solver.** Original builds a global system without neighborhood selection. OpenEvolve introduces diagonal regularization ( $10^{-10}$ ) and a pseudo-inverse fallback. OpenEvolve with GeoKnowledge is identical. GeoEvolve employs localized kriging using cKDTree nearest 25 neighbors and condition-number-adaptive regularization ( $10^{-10}\text{--}10^{-4}$ ), with mean fallback if the system is singular.

### A.10.3 KNOWLEDGE DISCOVERY FROM GEOEVOLVE

We summarize the key geospatial knowledge underlying the improved GeoEvolve algorithm, which can contribute to geospatial modeling.

**Expanded variogram family with automatic selection.** Fits appropriate smoothness and range, lowering RMSE/MAE and improving  $R^2$ .

**Adaptive empirical variogram (trimmed mean, quantile bins).** Stabilizes nugget/sill/range estimates and reduces run-to-run variance.

**Multi-start with parameter bounds in optimization.** Improves convergence and avoids negative or degenerate parameter estimates.

**Localized kriging with condition-based regularization.** Reduces computational cost (from  $O(n^3)$  to local operations) and improves robustness for ill-conditioned systems.

**Geo-knowledge injection.** Provides informative priors and narrows the search space, improving small-sample and non-stationary performance.

1242 A.11 EVOLVED GEOCP MODEL  
12431244 A.11.1 GEOEVOLVE-GEOCP (OUR MODEL)  
12451246 The fundamental conformal construction is preserved, but the following modifications are intro-  
1247 duced:1248 • **Refined geographic weighting.** While keeping the Gaussian kernel form  
1249

1250 
$$w_i(u_{\text{test}}, v_{\text{test}}) = \frac{\exp\left[-\frac{1}{2}\left(\frac{d((u_{\text{test}}, v_{\text{test}}), (u_i, v_i))}{\sigma}\right)^2\right]}{\sum_{j=1}^m \exp\left[-\frac{1}{2}\left(\frac{d((u_{\text{test}}, v_{\text{test}}), (u_j, v_j))}{\sigma}\right)^2\right]}, \quad (18)$$
  
1251  
1252

1253 GeoEvolve reoptimizes the bandwidth parameter  $\sigma$  through multi-start global search and  
1254 adaptive clipping  
1255

1256 
$$\sigma \in [\sigma_{\min}, \sigma_{\max}], \quad (19)$$
  
1257

1258 ensuring both numerical stability and fidelity to local spatial heterogeneity.  
12591260 • **Enhanced weighted quantile computation.** GeoEvolve consolidates earlier adaptive  
1261 strategies into a simplified yet robust stepwise quantile estimator:  
1262

1263 
$$Q_{1-\varepsilon}^{\text{geo}} = \inf \left\{ q : \sum_{i=1}^m w_i(u_{\text{test}}, v_{\text{test}}) \mathbf{1}\{a_i \leq q\} \geq 1 - \varepsilon \right\}. \quad (20)$$
  
1264

1265 The algorithmic implementation uses improved vectorization and conditioning checks,  
1266 guaranteeing accuracy and scalability on large test sets.  
1267

## A.11.2 COMPARISON OF EVOLVED GEOCP FROM DIFFERENT MODELS

1268 We summarize the key technical elements of the different code-evolution algorithms.  
12691270 **Original GeoCP.** This version uses a fixed-bandwidth Gaussian kernel  $e^{-0.5d^2}$  without weight  
1271 normalization. It computes weighted quantiles with a *stepwise* rule, selecting the index where cumula-  
1272 tive weights exceed  $q$  without interpolation, and adopts the quantile level  $q = \lceil (1 - \alpha)(N + 1) \rceil / N$ ,  
1273 which is slightly conservative. Only the mean interval score is reported as the uncertainty metric.  
1274 As a result, the method may produce overly wide or miscalibrated intervals in regions with strong  
1275 spatial heterogeneity or sparse sampling.1276 **OpenEvolve.** This stage introduces adaptive bandwidth, dynamically adjusting kernel width for  
1277 each test location based on its  $k$ -nearest neighbor distance and row-wise distance dispersion. It re-  
1278 places the stepwise weighted quantile with interpolated weighted quantiles, avoiding discontinuous  
1279 interval endpoints.1280 **OpenEvolve with GeoKnowledge.** Here the bandwidth is eo-knowledge guided: per-test  $k$ -NN  
1281 bandwidths are clipped to the empirical range  $[0.05, 0.5]$ . Weight normalization ensures that each  
1282 test point's kernel weights sum to one, providing numerical stability and spatial consistency. The  
1283 quantile level is refined to  $q = (1 - \alpha)(N + 1) / N$  (without ceiling), reducing conservativeness  
1284 and shortening intervals. Furthermore, comprehensive UQ metrics are reported, including mean  
1285 interval length, empirical coverage, and deviation from nominal coverage. Overall, this stage further  
1286 shortens intervals and achieves near-nominal coverage while remaining robust at boundaries and in  
1287 sparse areas.1288 **GeoEvolve.** GeoEvolve–GeoCP remains faithful to the core conformal prediction framework while  
1289 sharpening spatial weighting and quantile estimation, the two pillars of interval construction. The  
1290 refined geographic weighting adaptively tunes bandwidth to local heterogeneity, ensuring that con-  
1291 formal scores reflect the true spatial dependence and avoid instability.  
12921293 A.11.3 KNOWLEDGE DISCOVERY FROM GEOEVOLVE  
12941295 We distill the geospatial knowledge that underlies the improved GeoCP algorithm produced by Geo-  
1296 Evolve.  
1297

1296 **Adaptive bandwidth.** This mechanism adjusts kernel width to local calibration-point density, pre-  
1297 venting overly wide intervals in dense regions and overly narrow ones in sparse regions. It drives  
1298 the interval score down and keeps empirical coverage near  $(1 - \alpha)$ .  
1299

1300 **Interpolated weighted quantile.** By eliminating discrete jumps when cumulative weights cross the  
1301 quantile threshold, this refinement produces smoother, more stable prediction interval endpoints and  
1302 lowers variance.  
1303

1304 **Refined quantile level without ceiling.** This adjustment avoids the conservative upward bias from  
1305 the ceiling function, shortens interval length, and keeps empirical coverage close to the nominal  
1306 level.  
1307  
1308  
1309  
1310  
1311  
1312  
1313  
1314  
1315  
1316  
1317  
1318  
1319  
1320  
1321  
1322  
1323  
1324  
1325  
1326  
1327  
1328  
1329  
1330  
1331  
1332  
1333  
1334  
1335  
1336  
1337  
1338  
1339  
1340  
1341  
1342  
1343  
1344  
1345  
1346  
1347  
1348  
1349